

Miocene high elevation and high relief in the Central Alps

Emilija Krsnik^{1,2}, Katharina Methner^{1,5}, Marion Campani¹, Svetlana Botsyun³, Sebastian G. Mutz³, Todd
5 A. Ehlers³, Oliver Kempf⁴, Jens Fiebig², Fritz Schlunegger⁶, Andreas Mulch^{1,2}

¹Senckenberg Biodiversity and Climate Research Centre (SBiK-F), Senckenberganlage 25, Frankfurt (Main), 60325, Germany

²Institute of Geosciences, Goethe University Frankfurt, Altenhöferallee 1, Frankfurt (Main), 60438, Germany

³Department of Geosciences, University of Tübingen, Schnarrenbergstr. 94-96, 72076 Tübingen, Germany

⁴Federal Office of Topography swisstopo, Geologische Landesaufnahme, Seftigenstr. 264, Wabern, 3084, Switzerland

10 ⁵Department of Geological Sciences, Stanford University, CA 94305, USA

⁶Institute of Geological Sciences, University of Bern, Baltzerstrasse 3, Bern, 3012, Switzerland

Correspondence to:

Emilija Krsnik

15 Senckenberg Biodiversity and Climate Research Centre (BiK-F), Senckenberganlage 25,

60325 Frankfurt/Main

0049 69 7542 1815

emilija.krsnik@senckenberg.de

20 **Content**

- Text SI1 (Age constraints)
- Text SI2 (Analytical procedures)
- Text SI3 (Paleoelevation reconstruction)
- SI4 Figures (Fig. SI1–SI3)
- 25 – SI5 Data tables (Table SI1–SI5, tables can be found in a separate EXCEL file)

This supplementary information provides details on calculation of sample ages (SI1), analytical procedures (SI2), paleoelevation reconstruction (SI3), listed stable ($\delta^{13}\text{C}$, and $\delta^{18}\text{O}$; Table SI1) and clumped isotope data (Δ_{47} ; Tables SI2–SI4), and paleoelevation calculation for alternative scenarios with different oxygen isotope lapse rates and near sea level reference
30 baselines (Table SI5). It further comprises three additional figures showing pedogenic carbonate $\delta^{13}\text{C}$ values for each section (Fig. SI1), pedogenic carbonate $\delta^{18}\text{O}$ and $\delta^{13}\text{C}$ values as function of time for each section (Fig. SI2) and the $\delta^{18}\text{O}/\delta^{13}\text{C}$ relationship for the Aabach section (Fig. SI3). Data tables contain sample and age information, analytical results of oxygen and carbon stable isotope analysis for carbonate nodules, and calculated oxygen isotope data for meteoric water (Table SI1).

SII Age constraints for Fontannen, Jona, and Aabach sections

35 Pedogenic carbonate nodules from all three Swiss Molasse Basin sections were collected along magnetostratigraphically-dated sections and each sample was assigned an exact position within the local paleomagnetic stratigraphy. Age constraints for the Fontannen section follow the age model published in (Methner et al., 2020) and details on the calculation can be found therein. Chronostratigraphic framework for both, the Jona and Aabach sections has been established based on combined magnetostratigraphy (Kälin and Kempf, 2009; Kempf et al., 1997; Kempf and Matter, 1999), biostratigraphy (Bolliger, 1992; 40 Kälin, 1997), and radiometric dating of volcanic ashes (Gubler et al., 1992; Schmieder et al., 2018).

The Jona section spans an age interval of ca. 16.5 to 13.5 Ma (Kempf et al., 1997) and is dated by the projected Küsnacht bentonite (14.91 ± 0.09 Ma) and seven mammal sites comprising faunal zones MN 4b, MN 5, and MN 6. Furthermore, the Hüllistein conglomerate serves as an important stratigraphic marker bed (at 16 Ma; Kempf et al., 1997) and allows a lateral correlation with the Meilen limestone in the Aabach section 20 km further to the west (Kempf & Matter, 1999). We used the 45 paleomagnetic section of (Kempf et al., 1997) to construct the age model of the sampled section. We sampled ca. 650 m of the section covering the uppermost part of Chron C5Cr to the lowermost part of Chron C5ABr, spanning a time interval of 16.773 Ma to 13.711 Ma (chron ages from the Astronomically Tuned Neogene Time Scale (ATNTS2012; Hilgen et al., 2012).

Paleomagnetostratigraphy and age assignments for the Aabach section are presented in Kempf & Matter (1999). Absolute age constraints are given by two projected volcanic ash layers (the Küsnacht and the Urdorf bentonites) which are dated to 50 14.91 ± 0.09 Ma and 15.27 ± 0.12 Ma, respectively (Gubler et al., 1992). Biostratigraphic constraints include five mammal sites (all in mammal faunal zone MN 5; Kälin & Kempf, 2009). We sampled 352 m of the section covering the base of Chron C5Cr to the top of Chron C5Bn.1r, which transfers into a time interval of 17.222 Ma to 14.870 Ma (according to ATNTS2012; Hilgen et al., 2012). Uncertainties are introduced by two confirmed hiatuses at ~172 m and ~280 m of section with unknown durations. We defined the time of ending of the hiatuses to be at the beginning of the subsequent confirmed chron. We therefore 55 indicate that the section sequence was interrupted from 16.472–15.974 Ma, and 15.160–15.0321 Ma by hiatus 1 and hiatus 2, respectively. A third, yet unconfirmed hiatus is assumed at ~180 m of section and was therefore not considered in our age model.

Sample age error results from uncertainties of sample placement within the stratigraphic section. We assumed a maximum uncertainty of ± 15 m. Based on the interval with the lowest sedimentation rate (Fontannen = 0.20 mm/ a; Jona = 0.10 mm/ a, 60 and Aabach = 0.12 mm/ a) and assuming a constant sedimentation rate this transfers into a maximum error for the Fontannen section of ± 80 kyr, for the Jona section of ± 150 kyr, and for the Aabach section of ± 120 kyr.

SI2 Analytical procedures

2.1 Stable ($\delta^{13}\text{C}$, $\delta^{18}\text{O}$) isotope analyses

High time resolution oxygen and carbon stable isotope ($\delta^{13}\text{C}$, $\delta^{18}\text{O}_c$) analysis on carbonates from the Fontannen section (MC-
65 -) was carried out at Leibniz University Hannover, Germany, and data was presented in (Campani et al., 2012). Details on analytical setup and error calculation can be found therein. We complemented the stable isotope record from (Campani et al., 2012) with additional 16 samples which were collected and analysed in 2017 (Table SII; 17 EK--). $\delta^{13}\text{C}$ and $\delta^{18}\text{O}_c$ analysis of pedogenic carbonates from the Jona and Aabach sections was performed at the Joint Goethe University–Senckenberg BiK-F Stable Isotope Facility Frankfurt, Germany. Carbonate nodules were drilled with a low-speed micro drill. 0.1 mg to 2.5 mg of
70 sample powder was digested with orthophosphoric acid at 72°C. After a reaction time of 90 min the evolved CO_2 gas was extracted by the Thermo Scientific GasBench II inlet system and isotope ratios were measured with a Thermo Scientific MAT 253 mass spectrometer. International and in-house standard materials (Carrara, NBS-18, and Merck) were measured along with the samples. The isotopic results were reported in standard delta notation relative to VSMOW ($\delta^{18}\text{O}$) and VPDB ($\delta^{13}\text{C}$). Two standard errors ($2\sigma_n$) were calculated for each section based on the Carrara standard ($n_{\text{Fontannen}} = 22$; $n_{\text{Jona}} = 84$; $n_{\text{Aabach}} =$
75 56) and vary between 0.01 and 0.03‰ for $\delta^{18}\text{O}$ and between 0.01 and 0.02‰ for $\delta^{13}\text{C}$ (Table SII).

2.2 Carbonate clumped isotope (Δ_{47}) analyses

Carbonate clumped isotope analysis measures the extent to which the rare isotopes ^{13}C and ^{18}O are bound to one another within the carbonate mineral lattice forming the $^{13}\text{C}^{18}\text{O}^{16}\text{O}_2^{-2}$ ion group. Proportions of the ^{13}C – ^{18}O bonds (clumping) are sensitive to the carbonate formation temperature and are independent of the isotopic composition of the meteoric fluid from which the
80 carbonate grew (Eiler, 2011; and ref. therein). Clumped isotope values are reported as the variable “ Δ_{47} ” which is the difference, in per mil, between the measured abundance of the CO_2 isotopologue and the theoretical abundance of that isotopologue expected for a stochastic distribution of C and O isotopes for that sample. The Δ_{47} value can be expressed as:

$$\Delta_{47} = [(R^{47}/R^{47*} - 1) - (R^{46}/R^{46*} - 1) - (R^{45}/R^{45*} - 1)] * 1000 (\text{‰}) \quad (1)$$

where R^i is mass i /mass 44.

85 Carbonate clumped isotope analyses for 2013–2018 were performed on a Thermo Scientific MAT 253, and data for 2019 on a ThermoFisher 253 plus gas source isotope ratio mass spectrometer at the Joint Goethe University–Senckenberg BiK-F Stable Isotope Facility Frankfurt, Germany.

Sample powder was reacted with >106 % H_3PO_4 at 90°C for 30 min. Acid digestion, purification of extracted CO_2 gases, and measurements followed outlines provided by (Wacker et al., 2013, 2014), and (Bajnai et al., 2018).

90 The data has been acquired in five measurement periods (14.02.2013–28.03.2013; 03.05.2016–04.07.2016; 06.01.2017–10.07.2017; 10.07.2018–19.10.2018; 15.03.2019–05.08.2019).

Fontannen section

95 Δ_{47} values for the Fontannen section were measured in 2013 and 2016/2017 and were published in Methner et al. (2020). The details for the background correction can be found therein. Further data processing follows the same steps as for data obtained after 2017 (see paragraph “Jona and Aabach sections”).

Jona and Aabach sections

100 Δ_{47} values for the Jona and Aabach section were measured in 2018/2019. For samples measured in 2018 a background correction was accomplished by correcting directly for the contribution of secondary electrons to the m/z 47 raw signals by scaling the negative background of m/z 47 to the intensity of m/z 49 ion beam (Fiebig et al., 2016). Whenever the merged equilibrated gas data set displayed a non-zero slope in δ^{47} vs Δ_{47} space, the residual slope of the merged set of equilibrated gases was used to perform a final correction, according to the principle outlined by Dennis et al. (2013). Since January 2019
105 background correction was performed by monitoring the intensities measured on the m/z 47.5 cup according to the protocol outlined by Fiebig et al. (2019). The m/z 47.5 cup intensities was multiplied by a unique scaling factor of -1 and finally added to the intensities measured on the m/z 47 cup. After this background correction, equilibrated gases displayed a slope of zero in δ^{47} - Δ_{47} space, demonstrating that the non-linearity had been effectively removed.

The scale compression was monitored by measuring reference gases equilibrated at 1000°C and 25°C along with the carbonate
110 samples and carbonate reference materials (ETH1, ETH2, ETH3, ETH4, Carrara marble, and the aragonitic bivalve *A. islandica*). Empirical transfer function were determined by the comparison of nominal CDES-values of 0.9196 ‰ and 0.0266 ‰ for CO₂ equilibrated at 25 °C and 1000 °C, respectively, (Petersen et al., 2019) with the intercepts displayed by these gases in δ^{47} - Δ_{47} space. Finally, we applied an acid fractionation factor of +0.088‰ (Petersen et al., 2019) such that all Δ_{47} data is reported on the CDES 25 (Carbon Dioxide Equilibrium Scale at a reaction temperature of 25 °C).

115 Raw data were obtained on the basis of 10 acquisitions before 2019, and on 13 acquisitions since January 2019. Each acquisition consisted of 10 cycles with integration times of 20 seconds each. All data, including that of the Fontannen section, was processed with the IUPAC/ [BRAND] set of isotopic parameters ($^{13}\text{R}_{\text{VPDB}} = 0.011180$, $^{17}\text{R}_{\text{VSMOW}} = 0.038475$, $^{18}\text{R}_{\text{VSMOW}} = 0.0020052$, $\lambda = 0.528$; Daëron et al., 2016). Reference gases equilibrated at 1000°C and 25°C and associated empirical transfer functions (ETF) can be found in Table SI3.

120

Apparent carbonate formation temperatures were calculated using the following temperature calibration of (Petersen et al., 2019):

$$\Delta_{47}(\text{CDES } 25) = (0.0383 \pm 1.7\text{E}^{-6}) * (10^6 / T^2) + (0.258 \pm 1.7\text{E}^{-5}) \quad (2)$$

Each day we measured 1-3 carbonate reference materials along with the pedogenic carbonate samples. The mean $\Delta_{47}(\text{CDES})$
125 values (± 1 SD), averaged for the five measurement periods, are: Carrara (marble, calcite, $n = 264$) 0.406 (± 0.026) ‰, MuStd (*Arctica islandica*, aragonite, $n = 104$) 0.748 (± 0.021) ‰, Strauss ($n = 7$) 0.682 (± 0.024) ‰, ETH 1 (calcite, $n = 98$) 0.299

(±0.012) ‰, ETH 2 (calcite, n = 90) 0.300 (±0.015) ‰, ETH 3 (calcite, n = 101) 0.705 (±0.015) ‰, ETH 4 (calcite, n = 34) 0.538 (±0.014) ‰, and are listed separately for each measurement period in table SI4.

The external standard errors (1 SE) for 4–5 replicate measurements vary between 0.004 ‰ and 0.009 ‰.

130

2.3 Soil water oxygen isotopic composition

We calculated the oxygen ($\delta^{18}\text{O}_w$) isotopic composition of the soil (meteoric) water from which the pedogenic carbonate formed for each Swiss Molasse Basin carbonate sample and list the results in Table SI1 in the Supplementary Material. $\delta^{18}\text{O}_w$ values were calculated from $\delta^{18}\text{O}_c$ values by applying the measured Δ_{47} -based carbonate formation temperatures and the calcite-water fractionation equation of (Kim and O’Neil, 1997). Based on the revised acid fractionation factor (Kim et al., 2007), the updated calcite-water fractionation can be expressed as:

135

$$1000 \ln \alpha = 18.03 (1000/T) - 32.23 \quad (3)$$

where α is the fractionation factor and T is the fractionation temperature in kelvin. Note, that the original expression after Kim & O’Neil (1997) had a slightly different intercept of -32.42.

140

Additionally, we provide $\delta^{18}\text{O}_w$ values calculated after (Coplen, 2007) with the following equation:

$$1000 \ln \alpha = 17.4 (1000/T) - 28.6 \quad (4)$$

where α and T are the fractionation factor, respectively the fractionation temperature in kelvin.

145 SI3 Paleoelevation reconstruction

Paleoelevation estimates were derived from the relative difference in precipitation $\delta^{18}\text{O}_w$ values between the near sea level sites (Swiss Molasse Basin; SMB) and the high-elevation Simplon Fault Zone (SFZ) (Table SI5). For comparison we also show paleoelevation estimates for the Fontannen $\delta^{18}\text{O}_w$ record published in Campani et al. (2012) based on 1) a mean annual temperature of 21°C as derived from paleobotanical data (“Fontannen 2012”), and 2) the Δ_{47} -based carbonate formation temperature (“Fontannen”) as measured in this study. For near sea level precipitation $\delta^{18}\text{O}_w$ estimates we calculated the 1st quartile (lowest 25%) mean of the SMB $\delta^{18}\text{O}_w$ values averaged per horizons for the time interval 15.5–14.0 Ma (number of individual measurements $n_{\text{Fontannen}} = 47$; $n_{\text{Jona}} = 100$; $n_{\text{Aabach}} = 57$). Relative differences in precipitation $\delta^{18}\text{O}_w$ values ($\Delta(\delta^{18}\text{O}_w)$) between near sea level SMB and the high-elevation SFZ were calculated according to

150

$$\Delta(\delta^{18}\text{O}_w) = \delta^{18}\text{O}_w (\text{SFZ}) - \delta^{18}\text{O}_w (\text{SMB}) \quad (5)$$

In the next step, $\Delta(\delta^{18}\text{O}_w)$ values were converted into relative elevation differences based on four different isotope lapse rates. Campani et al. (2012) describes a regional oxygen isotope lapse rate of -0.20 ‰/ 100 m averaged for the northern and southern Alps. This lapse rate is very similar to the proposed one for Europe by (Poage and Chamberlain, 2001; -0.21‰/ 100 m). For

155

comparison we also give paleoelevations calculated with the ECHAM5-wiso iGCM oxygen isotope lapse rate (Botsyun et al., 2020; -0.24‰/ 100 m) and the thermodynamic model based lapse rate after (Rowley et al., 2001) (see also Rowley and
160 Garzione, 2007) which was defined in (Currie et al., 2005) as:

$$h = (-6.14 * 1/1000) \Delta(\delta^{18}\text{O}_w)^4 - 0.6765\Delta(\delta^{18}\text{O}_w)^3 - 28.623\Delta(\delta^{18}\text{O}_w)^2 - 650.66\Delta(\delta^{18}\text{O}_w) \quad (6)$$

where h describes the altitude difference between the near sea elevation and the high-elevation sites.

Error calculation

165 The propagated paleoelevation error is composed of combined errors of oxygen isotope composition analyses for the low-
elevation sites precipitation (SMB $\delta^{18}\text{O}_w$), the high-elevation site precipitation (SFZ $\delta^{18}\text{O}_w$), the SMB Δ_{47} -based carbonate
formation temperatures, and the error of the oxygen isotope lapse rate (here we restrict only to the regional isotope lapse rate
of $-0.2 \pm 0.04\text{‰}/ 100 \text{ m}$ given in Campani et al., 2012). We calculated a paleoelevation estimate error of $\pm 870 \text{ m}$ for the
obtained relative elevation difference based on the SMB Fontannen section, of $\pm 770 \text{ m}$ and $\pm 520 \text{ m}$ based on the SMB Jona
170 and Aabach sections, respectively (Table SI5).

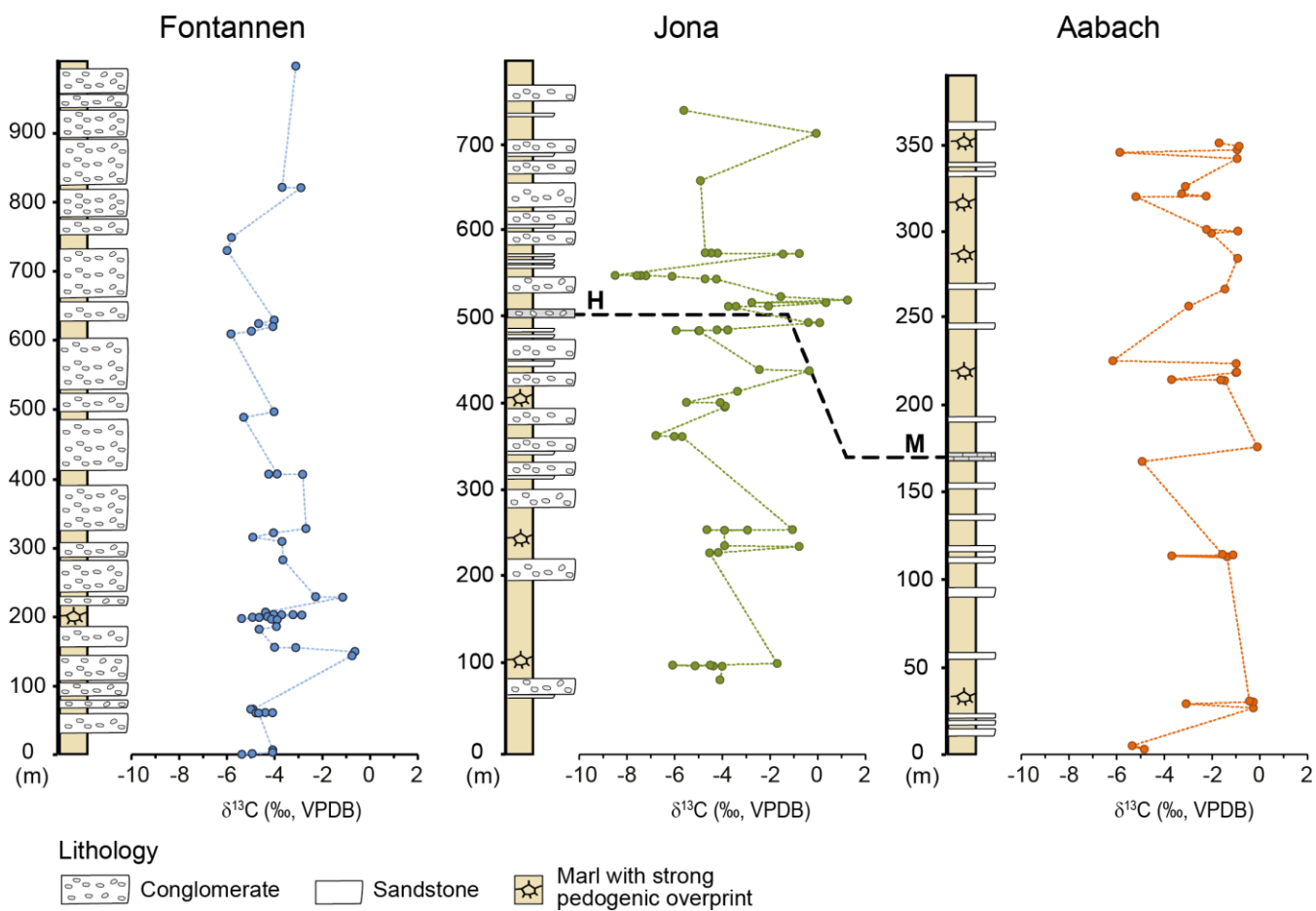


Figure SII: Pedogenic carbonate $\delta^{13}\text{C}$ values for Swiss Molasse Basin sections Fontannen, Jona, and Aabach. In total, 141 individual carbonate nodules were analyzed for Fontannen, respectively Jona, and 101 for Aabach. Only the mean value for each carbonate bearing horizon is shown here (Fontannen $n=50$; Jona $n=56$; Aabach $n=34$). Also shown is the stratigraphic position of the Hüllistein marker bed (H) and its equivalent for distal regions, the Meilen Limestone (M).

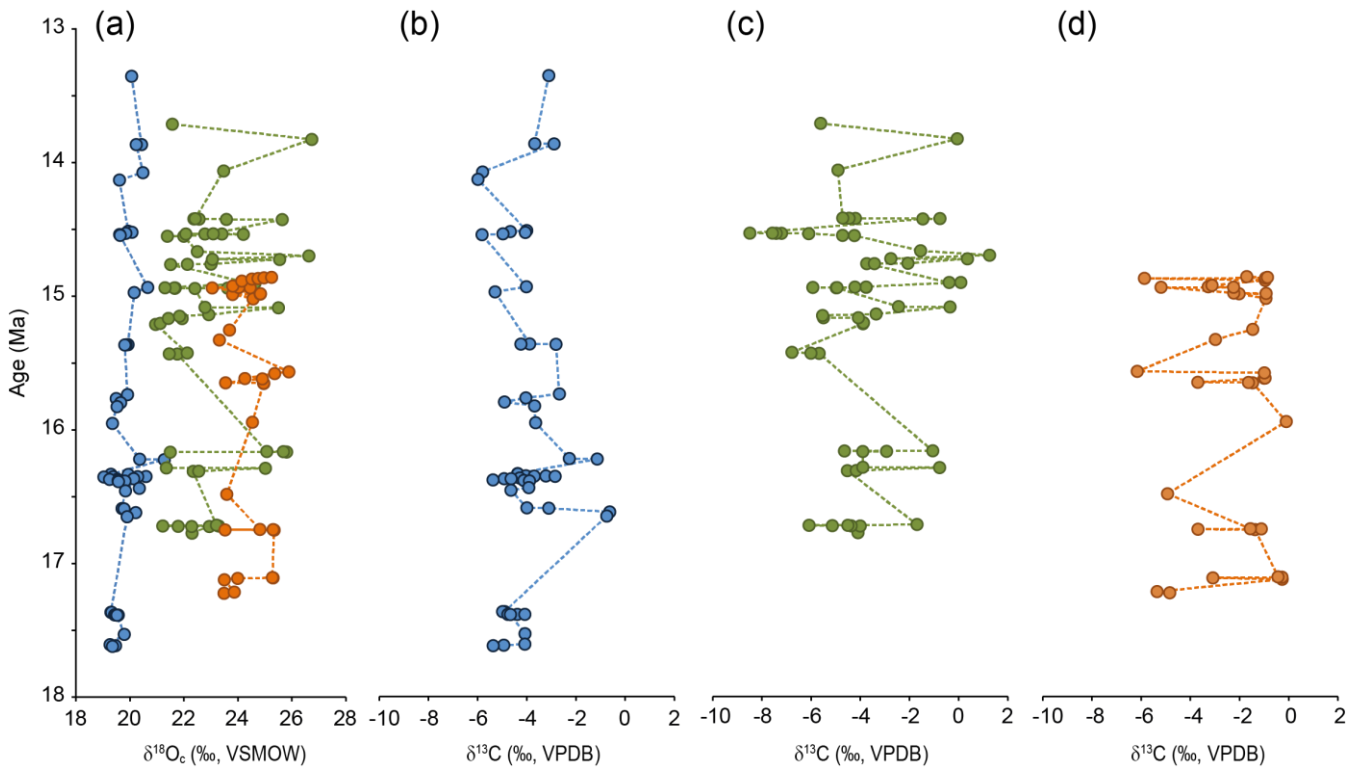
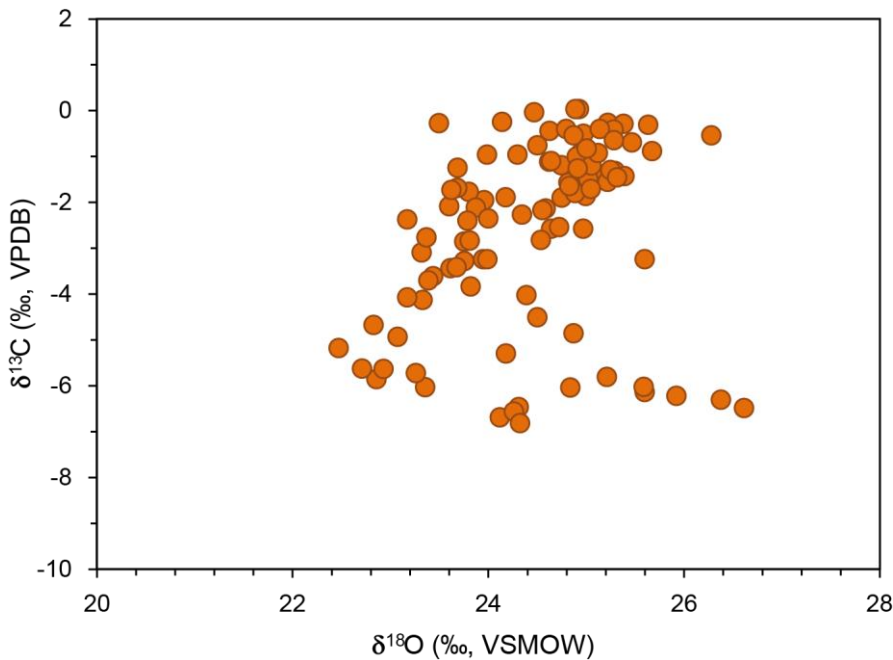


Figure SI2: Pedogenic carbonate $\delta^{18}\text{O}$ and $\delta^{13}\text{C}$ values of the Swiss Molasse Basin sections plotted against their ages. We show only the mean value for each carbonate bearing horizon. A) $\delta^{18}\text{O}$ values of the sections Fontannen (blue circles), Jona (green circles) and Aabach (orange circles). B–C) For purposes of visualization pedogenic carbonate $\delta^{13}\text{C}$ values are shown separately for each section (B: Fontannen, C: Jona, and D: Aabach).

180



185 **Figure SI3: Pedogenic carbonate $\delta^{18}\text{O}$ vs. $\delta^{13}\text{C}$ values for the Swiss Molasse Basin section Aabach. Shown are individual values for the section ($n = 101$). For the main part of the Aabach section samples show a covariant distribution between $\delta^{18}\text{O}$ and $\delta^{13}\text{C}$ values which we link to local environmental conditions prevailing in the distant megafan setting of this section. A positive correlation is typically found in pedogenic carbonates formed during dry conditions, when soil water evaporation and water stress in plants are intensified. Such conditions promote a positive bias in $\delta^{18}\text{O}$, which can lead to an overestimation of the paleoelevation. We therefore exclude the Aabach section as a suitable low elevation reference section for paleoelevation calculation.**

190

SI5 Data tables ($\delta^{18}\text{O}$, $\delta^{13}\text{C}$, Δ_{47})

Data tables can be found in a separate EXCEL file accompanying this manuscript and supplementary information.

Table SI1

195 Pedogenic carbonate oxygen ($\delta^{18}\text{O}$, VSMOW, ‰) and carbon ($\delta^{13}\text{C}$, VPDB, ‰) stable isotope values and calculated oxygen ($\delta^{18}\text{O}_w$, VSMOW, ‰) isotope values for meteoric (soil) water.

Table SI2

Clumped isotope compositions (δ^{47} , Δ_{47}) for pedogenic carbonate samples, empirical transfer function (ETF) for the respective periods of application, and derived carbonate formation temperatures following Petersen et al. (2019).

Table SI3

- 200 Measured δ^{47} (‰) and Δ_{47} (‰) values of CO₂ gases equilibrated at 1000°C (“heated gases”, “HG”) and at 25°C (“25G”) used for calculation of the empirical transfer function (ETF) for the respective periods of application.

Table SI4

Δ_{47} values (in ‰) for standard material listed for respective time intervals of clumped isotope measurements.

Table SI5

- 205 Calculated paleoelevation differences Δz (m) between low-elevation Swiss Molasse Basin (SMB) sections Fontannen and Jona and high-elevation Simplon Fault Zone (SFZ) for the time interval 15.5 Ma–14.0 Ma.

References

- Bajnai, D., Fiebig, J., Tomašových, A., Milner Garcia, S., Rollion-Bard, C., Raddatz, J., Löffler, N., Primo-Ramos, C. and Brand, U.: Assessing kinetic fractionation in brachiopod calcite using clumped isotopes, *Sci. Rep.*, 8(1), 1–13, doi:10.1038/s41598-017-17353-7, 2018.
- 210 Bolliger, T.: Kleinsäugerstratigraphie in der Miozänen Hörnlichschüttung (Ostschweiz), *Doc. naturae* 75., 1–296, 1992.
- Botsyun, S., Ehlers, T. A., Mutz, S. G., Methner, K., Krsnik, E. and Mulch, A.: Opportunities and Challenges for Paleoaltimetry in “Small” Orogens: Insights From the European Alps, *Geophys. Res. Lett.*, 47(4), doi:10.1029/2019GL086046, 2020.
- Campani, M., Mulch, A., Kempf, O., Schlunegger, F. and Mancktelow, N.: Miocene paleotopography of the Central Alps, 215 *Earth Planet. Sci. Lett.*, 337–338, 174–185, doi:10.1016/j.epsl.2012.05.017, 2012.
- Coplen, T. B.: Calibration of the calcite-water oxygen-isotope geothermometer at Devils Hole, Nevada, a natural laboratory, *Geochim. Cosmochim. Acta*, 71(16), 3948–3957, doi:10.1016/j.gca.2007.05.028, 2007.
- Currie, B. S., Rowley, D. B. and Tabor, N. J.: Middle Miocene paleoaltimetry of southern Tibet: Implications for the role of mantle thickening and delamination in the Himalayan orogen, *Geology*, 33(3), 181–184, doi:10.1130/G21170.1, 2005.
- 220 Eiler, J. M.: Paleoclimate reconstruction using carbonate clumped isotope thermometry, *Quat. Sci. Rev.*, 30(25–26), 3575–3588, doi:10.1016/j.quascirev.2011.09.001, 2011.
- Fiebig, J., Hofmann, S., Löffler, N., Lüdecke, T., Methner, K. and Wacker, U.: Slight pressure imbalances can affect accuracy and precision of dual inlet-based clumped isotope analysis, *Isotopes Environ. Health Stud.*, 52(1–2), 12–28, doi:10.1080/10256016.2015.1010531, 2016.
- 225 Gubler, T., Meier, M. and Oberli, F.: Bentonites as time markers for sedimentation of the Upper Freshwater Molasse: geological observations corroborated by high-resolution single-Zircon U-Pb ages., *Jahresversammlung der Schweizerischen Akad. der Naturwissenschaften*, (172), 12–13, 1992.
- Hilgen, F. J., Lourens, L. J., Van Dam, J. A., Beu, A. G., Boyes, A. F., Cooper, R. A., Krijgsman, W., Ogg, J. G., Piller, W. E.

- and Wilson, D. S.: *The Neogene Period.*, 2012.
- 230 Kälın, D.: The Mammal zonation of the Upper Marine Molasse of Switzerland reconsidered. A local biozonation of MN 2-MN 5, Aguilar, J.-P., Legendre, S., Michaux, J. (Eds.), *Actes du Congrès Biochrom'97. Mémoires. Trav. E.P.H.E. Montpellier* 21 *Biochrom'97*, 21(January 1997), 515–535, 1997.
- Kälın, D. and Kempf, O.: High-resolution stratigraphy from the continental record of the Middle Miocene Northern Alpine Foreland Basin of Switzerland, *Neues Jahrb. für Geol. und Paläontologie - Abhandlungen*, 254(1), 177–235, doi:10.1127/0077-235
- 7749/2009/0010, 2009.
- Kempf, O. and Matter, A.: Magnetostratigraphy and depositional history of the Upper Freshwater Molasse (OSM) of eastern Switzerland, *Eclogae Geol. Helv.*, 92(1), 97–103, doi:10.5169/seals-168650, 1999.
- Kempf, O., Bolliger, T., Kälın, D., Engesser, B. and Matter, A.: New magnetostratigraphic calibration of Early to Middle Miocene mammal biozones of the North Alpine foreland basin, in *Mémoires et travaux de l'Institut de Montpellier*, edited by
- 240 J.-P. Aguilar Legendre, S., Michaux, J., pp. 547–561, Montpellier., 1997.
- Kim, S.-T. and O'Neil, J. R.: Equilibrium and nonequilibrium oxygen isotope effects in synthetic carbonates, *Geochim. Cosmochim. Acta*, 61(16), 3461–3475, 1997.
- Kim, S. T., Mucci, A. and Taylor, B. E.: Phosphoric acid fractionation factors for calcite and aragonite between 25 and 75 °C: Revisited, *Chem. Geol.*, 246(3–4), 135–146, doi:10.1016/j.chemgeo.2007.08.005, 2007.
- 245 Methner, K., Campani, M., Fiebig, J., Löffler, N., Kempf, O. and Mulch, A.: Middle Miocene long-term continental temperature change in and out of pace with marine climate records, *Sci. Rep.*, 10(1), 1–10, doi:10.1038/s41598-020-64743-5, 2020.
- Petersen, S. V., Defliese, W. F., Saenger, C., Daëron, M., Huntington, K. W., John, C. M., Kelson, J. R., Bernasconi, S. M., Colman, A. S., Kluge, T., Olack, G. A., Schauer, A. J., Bajnai, D., Bonifacie, M., Breitenbach, S. F. M., Fiebig, J., Fernandez,
- 250 A. B., Henkes, G. A., Hodell, D., Katz, A., Kele, S., Lohmann, K. C., Passey, B. H., Peral, M. Y., Petrizzo, D. A., Rosenheim, B. E., Tripathi, A., Venturelli, R., Young, E. D. and Winkelstern, I. Z.: Effects of Improved 17O Correction on Interlaboratory Agreement in Clumped Isotope Calibrations, Estimates of Mineral-Specific Offsets, and Temperature Dependence of Acid Digestion Fractionation, *Geochemistry, Geophys. Geosystems*, 20(7), 3495–3519, doi:10.1029/2018GC008127, 2019.
- Poage, M. A. and Chamberlain, C. P.: Empirical relationships between elevation and the stable isotope composition of
- 255 precipitation and surface waters: Considerations for studies of paleoelevation change, *Am. J. Sci.*, 301(1), 1–15, 2001.
- Rowley, D. B. and Garzione, C. N.: Stable isotope-based paleoaltimetry, *Annu. Rev. Earth Planet. Sci.*, 35(January), 463–508, doi:10.1146/annurev.earth.35.031306.140155, 2007.
- Rowley, D. B., Pierrehumbert, R. T. and Currie, B. S.: A new approach to stable isotope-based paleoaltimetry: Implications for paleoaltimetry and paleohypsometry of the High Himalaya since the late Miocene, *Earth Planet. Sci. Lett.*, 188(1–2), 253–
- 260 268, doi:10.1016/S0012-821X(01)00324-7, 2001.
- Schmieder, M., Kennedy, T., Jourdan, F., Buchner, E. and Reimold, W. U.: A high-precision ⁴⁰Ar/³⁹Ar age for the Nördlinger Ries impact crater, Germany, and implications for the accurate dating of terrestrial impact events, *Geochim. Cosmochim. Acta*,

220, 146–157, doi:<https://doi.org/10.1016/j.gca.2017.09.036>, 2018.

Wacker, U., Fiebig, J. and Schöne, B.: Clumped isotope analysis of carbonates: comparison of two different acid digestion
265 techniques, *Rapid Commun. Mass Spectrom.*, 27, 1631–1642, doi:10.1002/rcm.6609, 2013.

Wacker, U., Fiebig, J., Tödter, J., Schöne, B. R., Bahr, A., Friedrich, O., Tütken, T., Gischler, E. and Joachimski, M. M.:
Empirical calibration of the clumped isotope paleothermometer using calcites of various origins, *Geochim. Cosmochim. Acta*,
141, 127–144, doi:10.1016/j.gca.2014.06.004, 2014.